SUPPORTING INFORMATION

Porous $NiTiO_3/TiO_2$ nanostructures for photocatatalytic hydrogen evolution

Congcong Xing,[ab] Yongpeng Liu,[c] Yu Zhang,[a] Junfeng Liu,[a] Ting Zhang,[d] Pengyi Tang,[d] Jordi Arbiol,[de] Lluís Soler,[b] Kevin Sivula,[c] Néstor Guijarro,[c] Xiang Wang,[a] Junshan Li,[a] Ruifeng Du,[a] Yong Zuo,[a] Andreu Cabot,*[ae] Jordi Llorca *[b]

a. Catalonia Institute for Energy Research (IREC), Sant Adrià de Besòs, 08930 Barcelona, Spain

b. Institute of Energy Technologies, Department of Chemical Engineering and Barcelona Research Center in Multiscale Science and Engineering, Universitat Politècnica de Catalunya, EEBE, 08019 Barcelona, Spain

c. Laboratory for Molecular Engineering of Optoelectronic Nanomaterials (LIMNO), École Polytechnique Fédérale de Lausanne (EPFL), Station 6, CH-1015 Lausanne, Switzerland

d. Catalan Institute of Nanoscience and Nanotechnology (ICN2), CSIC and BIST, Campus UAB, Bellaterra, 08193 Barcelona, Catalonia, Spain

e. ICREA, Pg. Lluis Companys 23, 08010 Barcelona, Spain

* *E-mails:* A. Cabot: *acabot@irec.cat*

J. Llorca: *jordi.llorca@upc.edu*

Content

1. Photoreactor

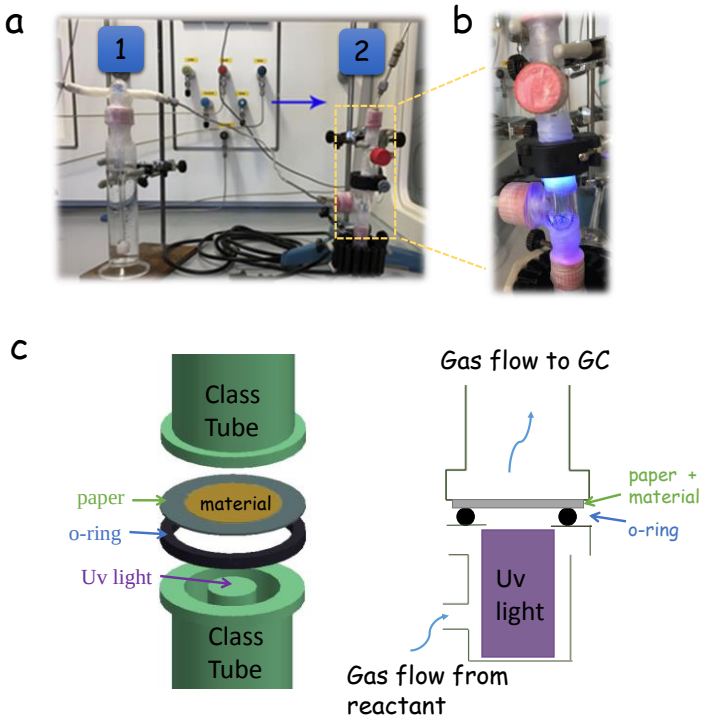

Figure S1. a) Photograph of the system used to test the photocatalytic hydrogen generation: 1 displays the Dreschel bottle containing the ethanol-water solution (1:9 molar). 2 displays the actual photoreactor. b) Scheme of the photoreactor.

2. Additional SEM characterization of the precursor materials

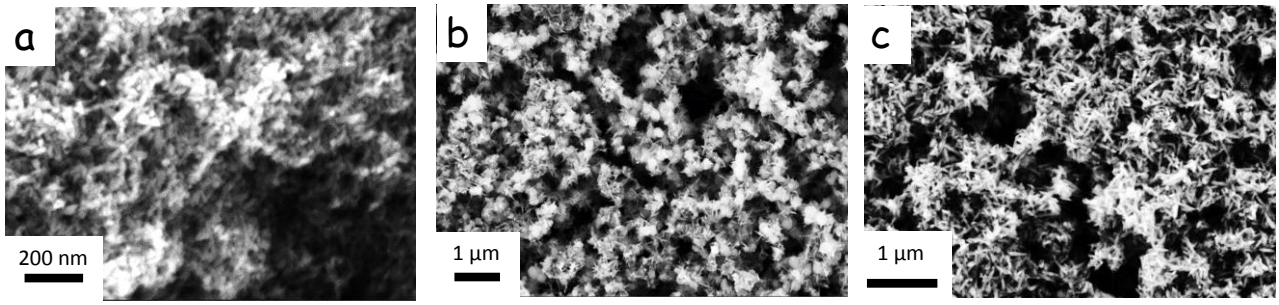

Figure S2. SEM images of TiO_2:Ni (5%) produced in the following conditions: a) without HDA, b) without H_2O, c) in HDA-H_2O-KCl.

3. Additional TEM characterization

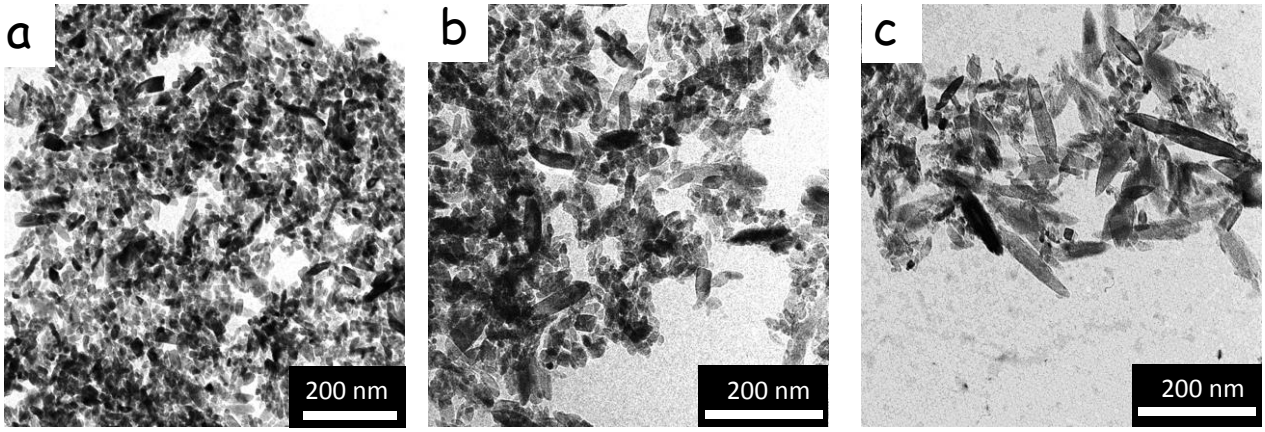

Figure S3. TEM images of (a) TiO_2, (b) TiO_2:Ni (1%), (c) TiO_2:Ni (2%).

4. Elemental composition

Table S1. Ti and Ni atomic concentrations of TiO_2, TiO_2:Ni (1%, 2%, 5%) and $NiTiO_3/TiO_2$ (1%, 2%, 5%). XRD data refers to the TiO_2 and $NiTiO_3$ crystallographic phases detected and it does not take into account any peak shift denoting the presence of Ni within the TiO_2 structure.

catalysts	EDX		XRD		XPS	
	Ti (atom%)	Ni (atom%)	Ti (atom%)	Ni (atom%)	Ti (atom%)	Ni (atom%)
TiO_2	100					
TiO_2:Ni (1%)	96.4	3.6			94.3	5.7
TiO_2:Ni (2%)	93.6	6.4				
TiO_2:Ni (5%)	83.2	16.8				
$NiTiO_3/TiO_2$ (1%)	96.4	3.6	4.4	95.6	94.2	5.8
$NiTiO_3/TiO_2$ (2%)	94.3	5.7	6.5	93.5		
$NiTiO_3/TiO_2$ (5%)	86	14	13.3	86.7		
$NiTiO_3$	61.9	39.1				

5. Scheme of the preparation procedure

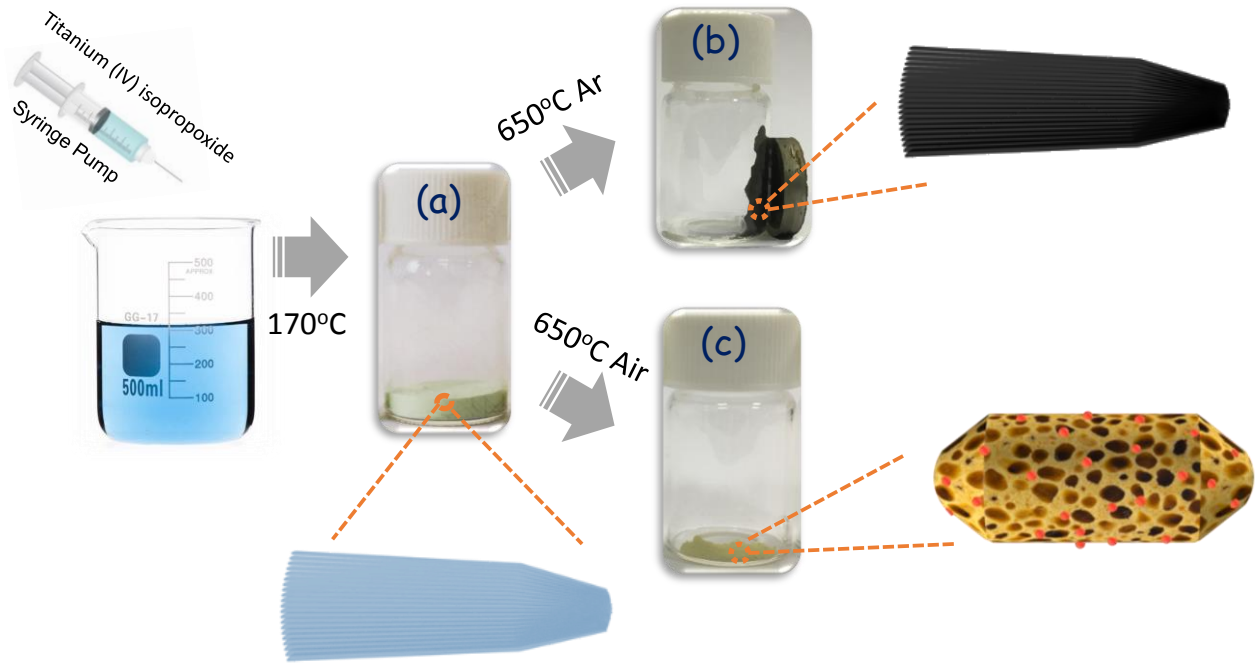

Figure S4. Scheme of the TiO_2:Ni precursor preparation procedure: (a) TiO_2:Ni, (b) NiO_x/TiO_2, (c) $NiTiO_3/TiO_2$.

6. EELS elemental maps and HRTEM of TiO_2

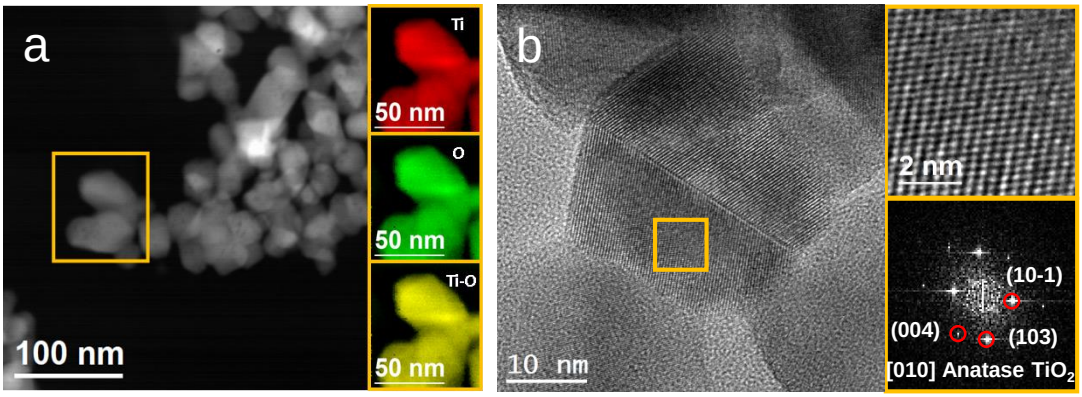

Figure S5. Undoped TiO_2 annealed at 650 °C in air: (a) STEM micrograph and EELS chemical composition maps obtained from the yellow squared area of the STEM micrograph. Individual Ti $L_{2,3}$-edges at 456 eV (red) and O K-edge at 532 eV (green) as well as its composite. (b) HRTEM micrograph, detail of the yellow squared region and its corresponding power spectrum.

7. XRD Rietveld refinement

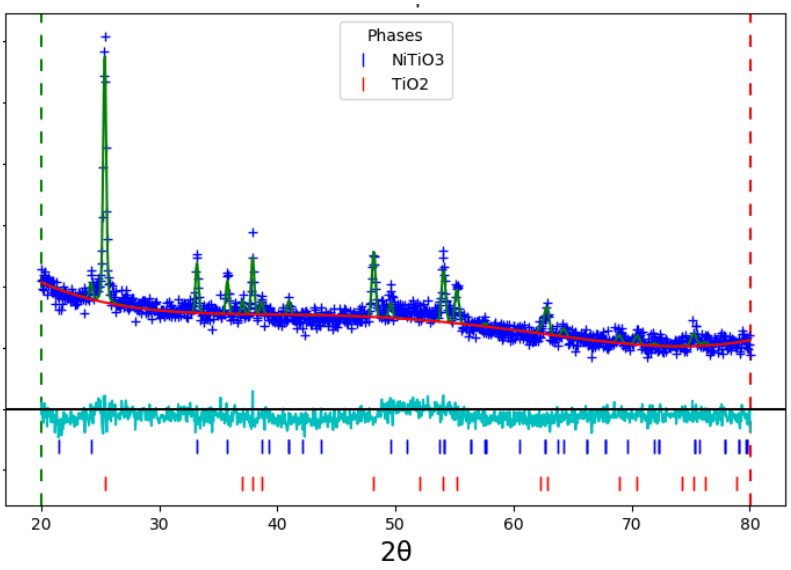

Figure S6 Refined fitting of the $NiTiO_3/TiO_2$(5%) x-ray diffraction data. Blue symbols: experimental data; continuous red line: modified background; continuous green line: calculated modelled structure; continuous light blue line beneath pattern: difference between observed and calculated parameters. Blue tickmarks correspond to reflections of $NiTiO_3$ (R-3) unit cell, lower red ones to TiO_2 (I41/amd) unit cell. GOF = 1.21. Rw = 6.99%.

8. HRTEM characterization of $NiTiO_3/TiO_2$ (1%)

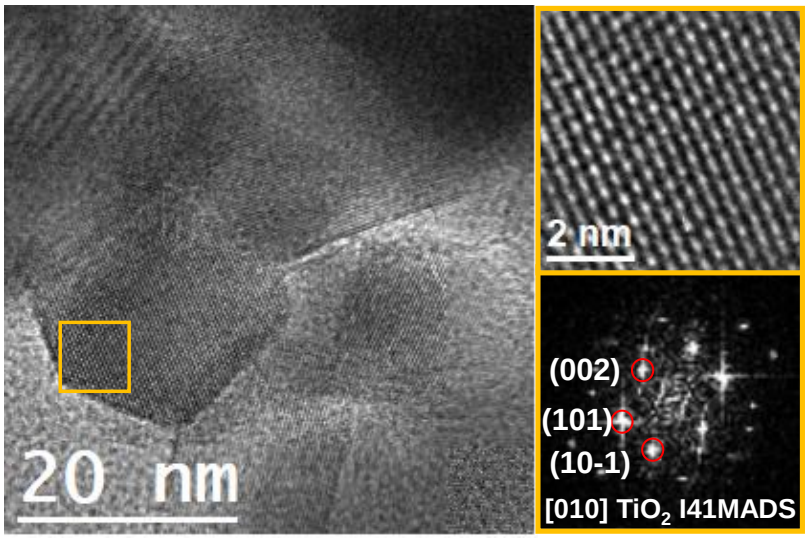

Figure S7 HRTEM micrographs of $NiTiO_3/TiO_2$ (1%), detail of the yellow squared region and its corresponding power spectrum.

9. XPS analyses

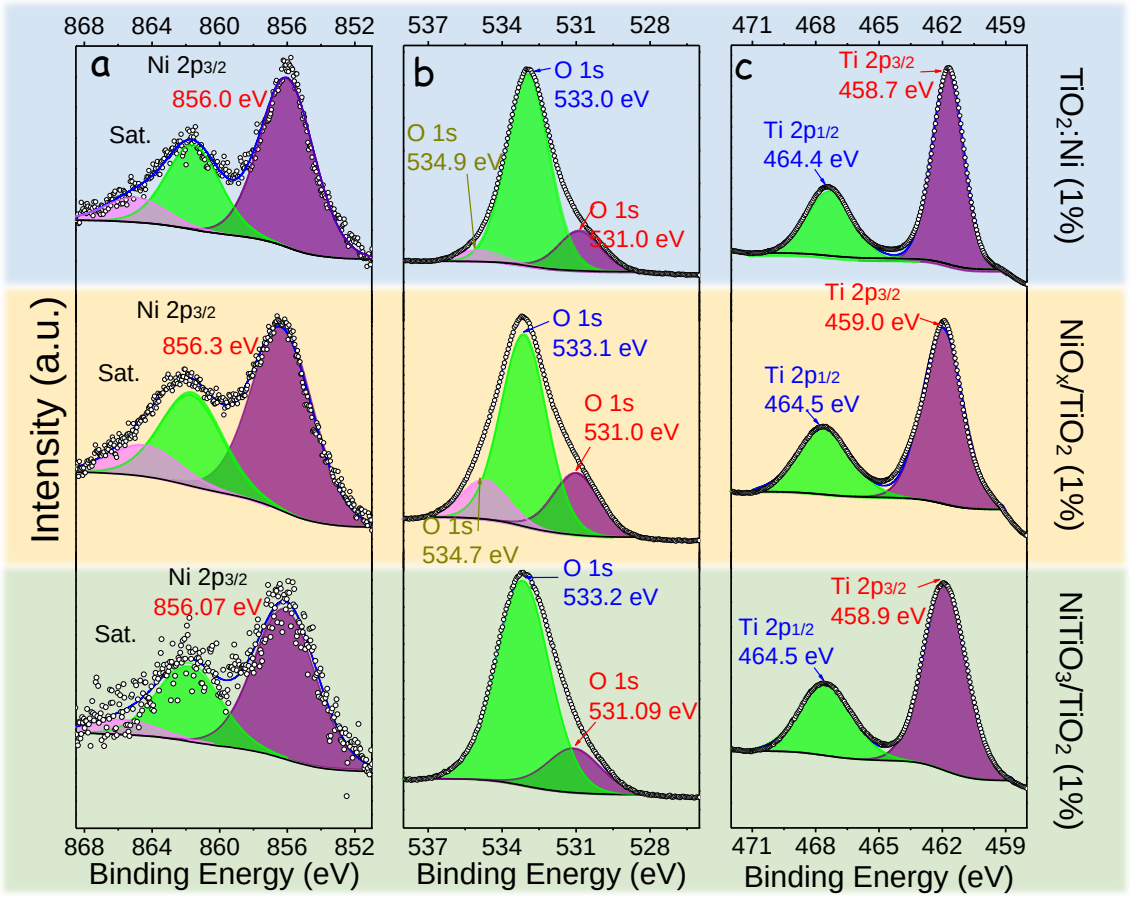

Figure S8. Ni $2p_{3/2}$ region (a), O 1s region (b) and Ti 2p region (c) of the XPS spectra of (1) TiO_2:Ni (1%) (2) NiO_x/TiO_2 (1%) and (3) $NiTiO_3/TiO_2$ (1%) samples.

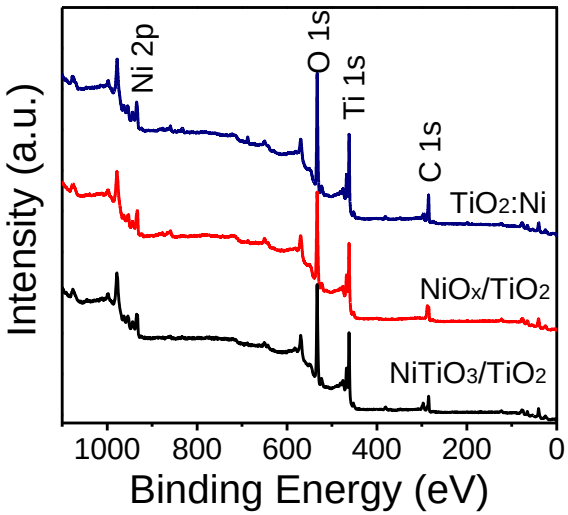

Figure S9. Survey XPS spectra of TiO_2:Ni (1%), NiO_x/TiO_2 (1%) and $NiTiO_3/TiO_2$ (1%).

10. TiO_2:Ni annealed in argon

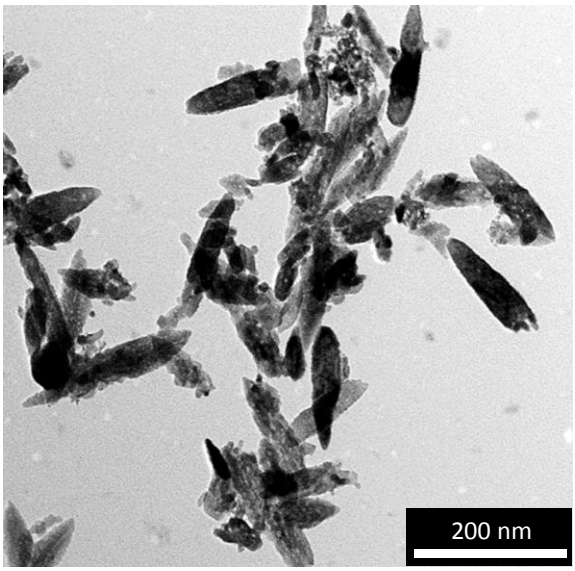

Figure S10. TEM image of NiO_x/TiO_2 (5%) annealed in argon.

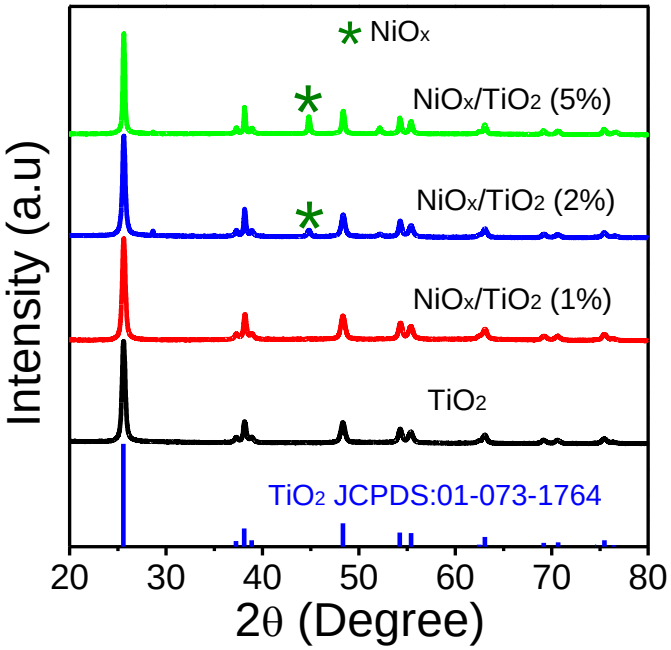

Figure S11. XRD pattern of TiO_2 and NiO_x/TiO_2 (1%, 2%, 5%) annealed in argon.

11.Nitrogen adsorption-desorption isotherms

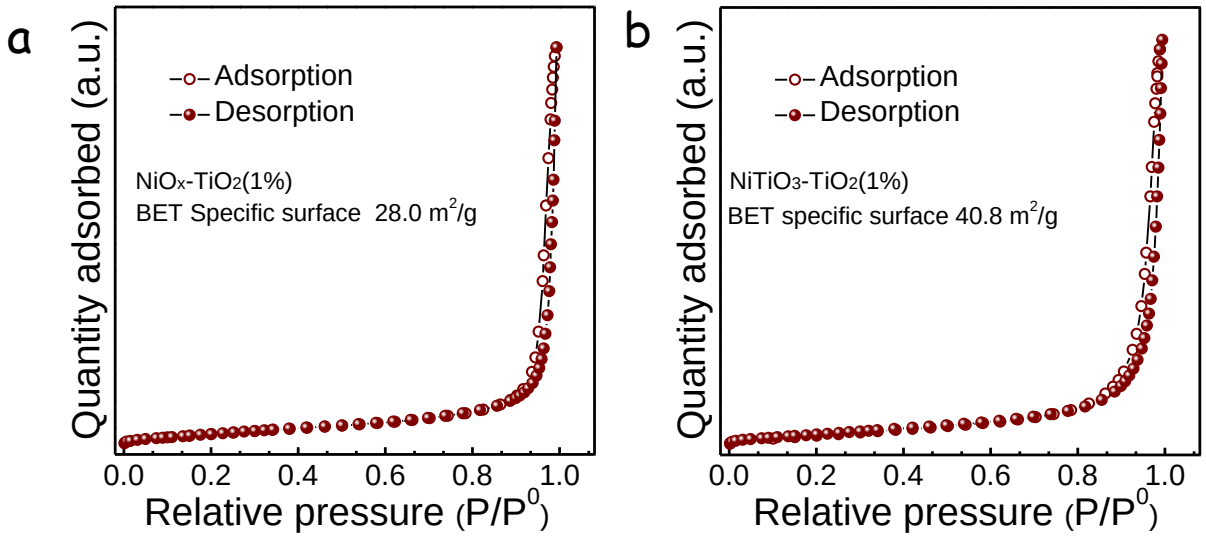

Figure S12. Nitrogen adsorption (open symbols) and desorption (filled symbols) isotherms measured of (a) NiO_x-TiO_2(1%) and (b) $NiTiO_3$-TiO_2(1%) at 77.3 K.

12. $NiTiO_3$ reference material

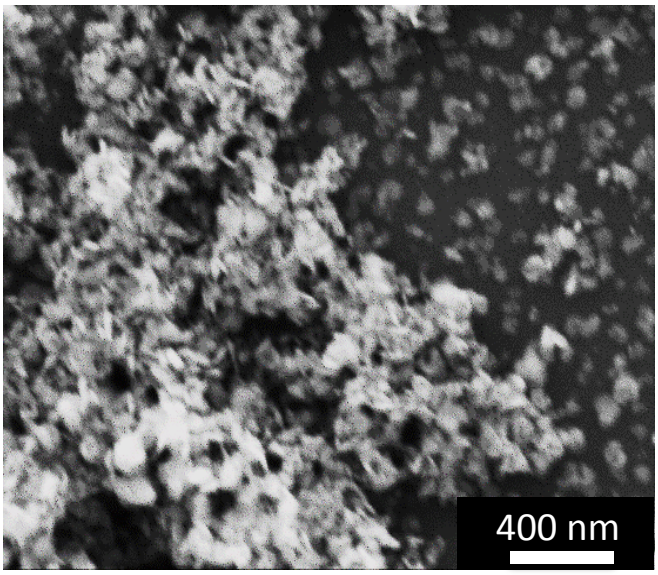

Figure S13. SEM images of $NiTiO_3$

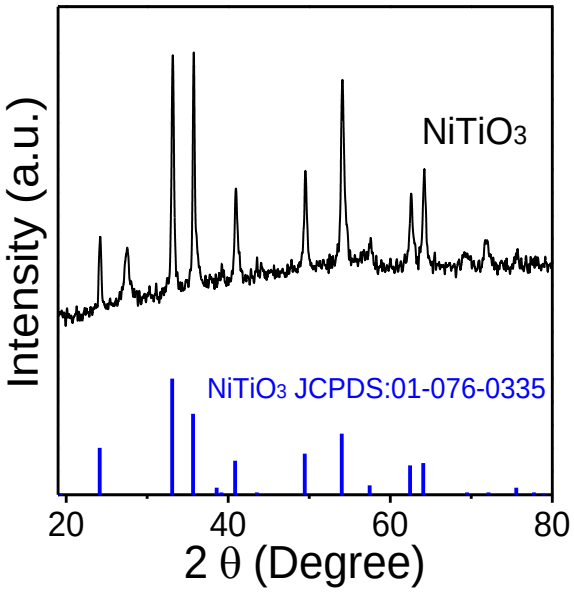

Figure S14. XRD pattern of $NiTiO_3$

13. Literature comparison

Table S2. Comparison of the hydrogen evolution rate and the apparent quantum yield with reported Ni-Ti-O systems.

Photocatalyst	H_2 Evolution Rate μmol h^{-1} g^{-1}	Reaction conditions	AQY %	Ref.
Ni/NiO/N-TiO_{2-x}	185	110W λ>420nm	7.5	S1
0.23%$Ni(OH)_2$ on TiO2	900	3W 365nm	12.4	S2
0.25wt% NiO-TiO_2	261	3W 365nm	1.7	S3
TiO_2-$Ni(HCO_3)_2$-2.5%	377	300W 380nm (±5nm)	6.24	S4
0.32% $Ni(NO_3)_2$-TiO_2	163	3W 365nm	8.1	S5
Mesoporous NiO/TiO_2	240	3W 365nm	1.7	S6
Pt NiO/$TiO_2$1:1 molar ratio	1,250	400W UV	7.8	S7
Hollow $NiTiO_3$/TiO_2(1%)	11,500	365nm	11.6	This work

14. Photocatalytic H_2 production rates

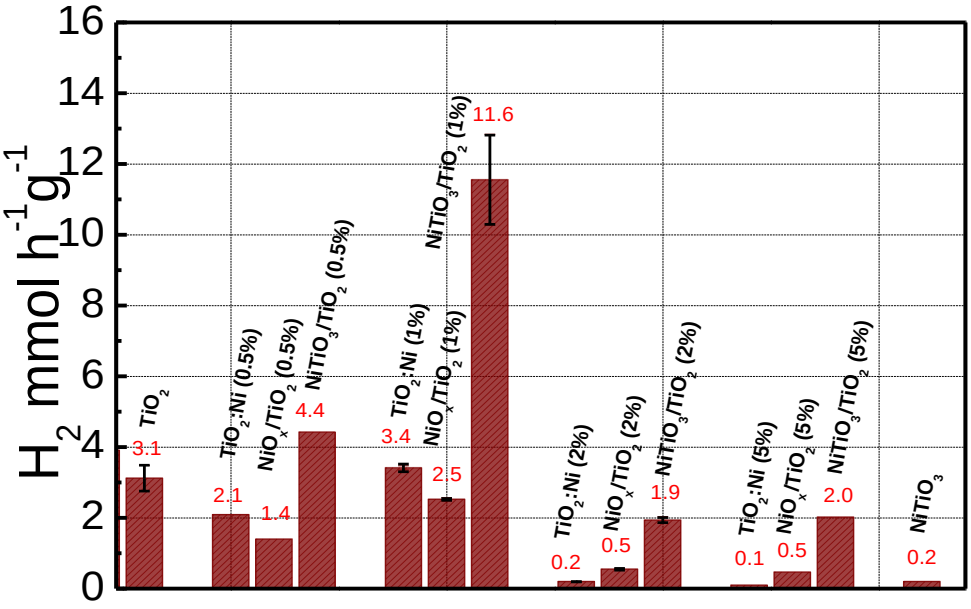

Figure S15. Photocatalytic H_2 production rates obtained from TiO_2, $NiTiO_3$, TiO_2:Ni (1%), NiO_x/TiO_2 (1%), $NiTiO_3/TiO_2$ (1%, 2%, 5%).

15.UV-vis analysis

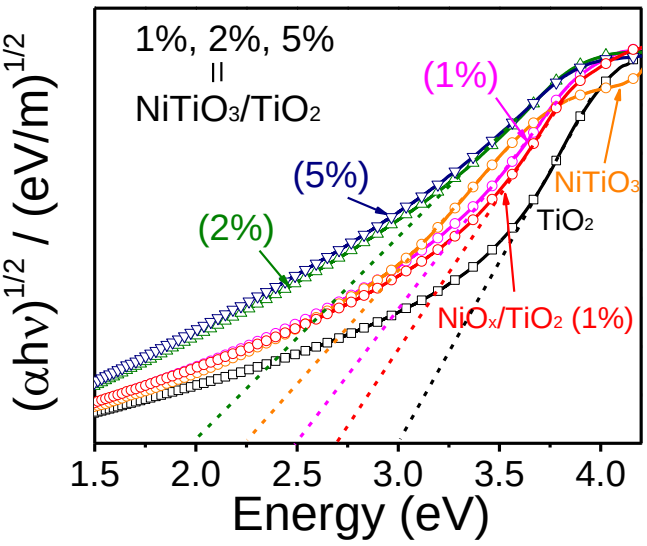

Figure S16. Kubelka-Munk function for TiO_2, $NiTiO_3/TiO_2$ (1, 2, 5%) and NiO_x/TiO_2 including a linear fit (dashed lines) to determine the band gap energy.

References

S1. S. Hu, F. Li, Z. Fan and J. Gui, *J. Power Sources*, 2014, **250**, 30–39.
S2. J. Yu, Y. Hai and B. Cheng, *J. Phys. Chem. C*, 2011, **115**, 4953–4958.
S3. L. Li, B. Cheng, Y. Wang and J. Yu, *J. Colloid Interface Sci.*, 2015, **449**, 115–121.
S4. Y. Wei, G. Cheng, J. Xiong, F. Xu and R. Chen, *ACS Sustain. Chem. Eng.*, 2017, **5**, 5027–5038.
S5. W. Wang, S. Liu, L. Nie, B. Cheng and J. Yu, *Phys. Chem. Chem. Phys.*, 2013, **15**, 12033–12039.
S6. L. Li, B. Cheng, Y. Wang and J. Yu, *J. Colloid. Interf. Sci.,* 2015, **449**, 115-121.
S7. A. Rawool, M. R. Pai, A. M. Banerjee, A. Arya, R. Ningthoujam, R. Tewari, R. Rao, B. Chalke, P. Ayyub and A. Tripathi, *Appl. Catal. B Environ.,* 2018, **221**, 443-458.